The transition between hole-pairs and four-hole clusters in four-leg t-J ladders

Thomas Siller [1], Matthias Troyer[1], T. M. Rice[1], Steven R. White[2]

1 *Theoretische Physik, Eidgenössische Technische Hochschule, CH-8093 Zürich, Switzerland*

[2] *Department of Physics and Astronomy, University of California Irvine, CA 92697*

(February 1, 2008)

Holes weakly doped into a four-leg t-J ladder bind in pairs. At dopings exceeding a critical doping of $\delta_c \simeq \frac{1}{8}$ four hole clusters are observed to form in DMRG calculations. The symmetry of the ground state wavefunction does not change and we are able to reproduce this behavior qualitatively with an effective bosonic model in which the four-leg ladder is represented as two coupled two-leg ladders and hole-pairs are mapped on hard core bosons moving along and between these ladders. At lower dopings, $\delta < \delta_c$, a one dimensional bosonic representation for hole-pairs works and allows us to calculate accurately the Luttinger liquid parameter K_ρ, which takes the universal value $K_\rho = 1$ as half-filling is approached.

I. INTRODUCTION

Strongly correlated electrons confined to move on ladders formed from coupled chains have been an active topic of research in recent years. These examples of lightly doped spin liquids can be very efficiently analyzed using the density matrix renormalization group [1,2] (DMRG) method, which allows long ladders to be accurately simulated. Ladders with an even number of legs have spin liquid groundstates at half-filling and the spin liquid character remains upon doping due to the binding of holes to form pairs at low concentrations [3–10]. The underlying physics of the ladder systems has close similarities to that of a doped resonant valence bond (RVB) phase which is widely believed to be realized in the high-T_c superconductors. The numerically accurate DMRG simulations of the strongly correlated t-J model [11] give a clear picture of the behavior of hole-pairs but only in qualitative terms as the density varies.

In this paper our aim is to analyze the DMRG results and to use them to determine the effective interactions between hole-pairs which govern their behavior. Since the spin sector of even leg ladders remains gapped, there are only charge degrees of freedom at low energies and these can be represented in terms of suitable hard core boson models. These in turn can be analyzed much more easily and completely. In an earlier paper [12] we described such a representation or mapping of the hole-pairs on a two-leg ladder to hard core bosons on a single chain. This enabled us to determine the effective repulsive interactions between the hard core bosons by fitting to the hole density distribution determined by DMRG for the t-J model. In the present paper we extend this analysis to four-leg ladders. The extra transverse degrees of freedom allow the formation of larger clusters of two hole-pairs (i.e. four hole clusters) when the hole density exceeds a critical concentration $\delta_c \simeq \frac{1}{8}$. A cluster represents not a bound state of the hole-pairs but a finite energy resonance which becomes populated when the chemical potential reaches a certain threshold.

The outline of the paper is as follows. First we treat the low concentration region where the density profiles

obtained from DMRG simulations show that hole-pairs simply repel each other. In this region we extend the mapping onto the model of hard core bosons that we used earlier for the two-leg ladder and obtain a parameterization of the repulsive interactions and Luttinger liquid exponent K_ρ. We compare the evolution of K_ρ with hole density in the two and four leg ladders. In both cases $K_\rho \to 1$ as the hole concentration $\delta \to 0$ indicating predominantly superconducting correlations. To treat the formation of the four hole clusters it is necessary to introduce additional transverse degrees of freedom. This is done by mapping the hole-pairs on a four-leg ladder onto a hard core boson model on a two-leg ladder. Choosing a potential with a repulsive tail but with a finite energy resonance on a single rung allows us to reproduce the DMRG results for the four-leg t-J model, both for the kink in the chemical potential and for the change in the density profile at the critical density. The paper ends with a concluding section.

II. HOLE PAIRS AND CLUSTERS

We consider the t-J ladder Hamiltonian

$$H = -t \sum_{\langle \mathbf{i},\mathbf{j} \rangle, \sigma} \mathcal{P}(c_{\mathbf{i}\sigma}^\dagger c_{\mathbf{j},\sigma} + c_{\mathbf{j},\sigma}^\dagger c_{\mathbf{i},\sigma})\mathcal{P} \qquad (1)$$
$$+ J \sum_{\langle \mathbf{i},\mathbf{j} \rangle}(\mathbf{S_i S_j} - \frac{1}{4}n_\mathbf{i} n_\mathbf{j})$$

for a four-leg ladder (4LL) configuration as depicted in Fig. 1. Here $\sigma = (\uparrow, \downarrow)$ denotes the spin index and $\langle \mathbf{i}, \mathbf{j} \rangle$ the summation over nearest-neighbor sites with $\mathbf{i} = (x, y)$ as site index. The operators $c_{\mathbf{i},\sigma}^\dagger$ and $c_{\mathbf{i},\sigma}$ create or destroy electrons with spin σ at position $\mathbf{i}$ respectively. The corresponding density operator is $n_{\mathbf{i},\sigma} = c_{\mathbf{i},\sigma}^\dagger c_{\mathbf{i},\sigma}$ and $n_\mathbf{i} = n_{\mathbf{i},\uparrow} + n_{\mathbf{i},\downarrow}$. The projection operator $\mathcal{P} \equiv \prod_\mathbf{i}(1 - n_{\mathbf{i},\uparrow} n_{\mathbf{i},\downarrow})$ prohibits double occupancy of a site and $\mathbf{S_i}$ denotes the spin at site $\mathbf{i}$. We use $J = 0.35\,t$ throughout. If not noted otherwise, we use the DMRG method to compute ground state properties which implies that open boundary conditions on the ends of the ladder are used.
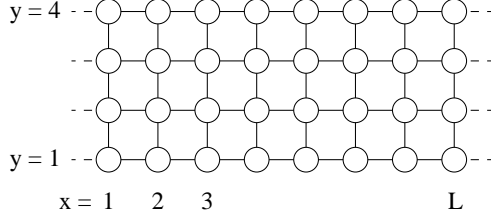
1

$y = 4$

$y = 1$

$x = 1 \quad 2 \quad 3 \qquad\qquad L$

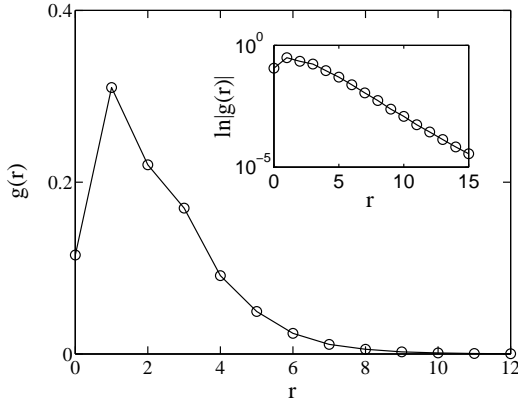FIG. 1. Indexing convention for a $(L \times 4)$ ladder.

FIG. 2. Hole-hole correlations $g(r)$ as a function of the relative separation r along the legs measured on a (32×4) ladder with two holes and $J = 0.35\,t$. The inset shows a logarithmic plot of the same data.

We start by examining the internal structure of a hole-pair (HP) on a t-J 4LL, by studying the hole-hole correlation (HHC) function. Since the DMRG computations are performed with open boundaries, special care must be taken in the measurement of the HHC-function, which we define as

$$g_{y,y'}(x, x') = \frac{\langle n^h_{x,y} \, n^h_{x',y'} \rangle}{\langle n^h_{x,y} \rangle \langle n^h_{x',y'} \rangle} \, n^h \ . \tag{2}$$

Here $n^h_{x,y} = 1 - n_{x,y}$ denotes the hole density operator acting on position (x, y) and n^h is the average hole density. Introducing relative and center of mass coordinates, $r = (0, 1, \ldots)$ and $R_0 = (1, 3/2, 2, \ldots)$ in the long direction, we define with

$$g(r, R_0) = \sum_{y,y'} g_{y,y'}(R_0 - \frac{r}{2}, R_0 + \frac{r}{2}) \tag{3}$$

the HHC between different rungs. To obtain a good approximation for the HHC function $g(r)$ on an infinite ladder, we measure $g(r, R_0)$ for an $(L \times 4)$ ladder in the middle of the system, i. e. for $R_0 \simeq L/2$. In this way we have measured $g(r)$ on a (32×4)-ladder with open boundaries. The result is plotted in Fig. 2. It shows clearly that in the ground state the two holes are bound. The correlation function decreases exponentially as can be seen from the logarithmic plot in the inset. The correlation length is 1.358 and hence larger than in the two-leg ladder (2LL) case where we have obtained 1.184 [12]. This suggests that the binding energy of a HP is reduced as the effective dimension is enhanced. With $E(N)$ as the ground state energy with N holes doped into the ladder we have computed the binding energy defined as

$$E_b = 2\,E(1) - E(0) - E(2) \tag{4}$$

for two and 4LL using systems with 40 and 24 rungs respectively. As expected, we have obtained a lower binding energy $E_b = 0.1062\,t$ for the 4LL than for the 2LL case, $E_b = 0.1487\,t$.

If the HP behave as hard core bosons (HCB) at low hole doping one should find as many maxima in the hole density profile of a t-J 4LL with open boundaries as the number of HP. In fact, we observe this only below a critical doping of $\delta_c \simeq \frac{1}{8}$ in contrast to the results obtained for two-leg ladders, [12] where this equality holds to much higher dopings. Figures 3 and 4 shows the hole density profiles for the groundstate of a (16×4) ladder for 2 up to 12 holes. The plot with 6 holes doped into the ladder corresponds to a hole density per site $\delta < \frac{1}{8}$ and shows three maxima as expected. For 8 holes doped into the ladder ($\delta = \frac{1}{8}$) we could expect to find four maxima, but we observe only three, suggesting that larger clusters of four holes are forming in some way as will be discussed later.
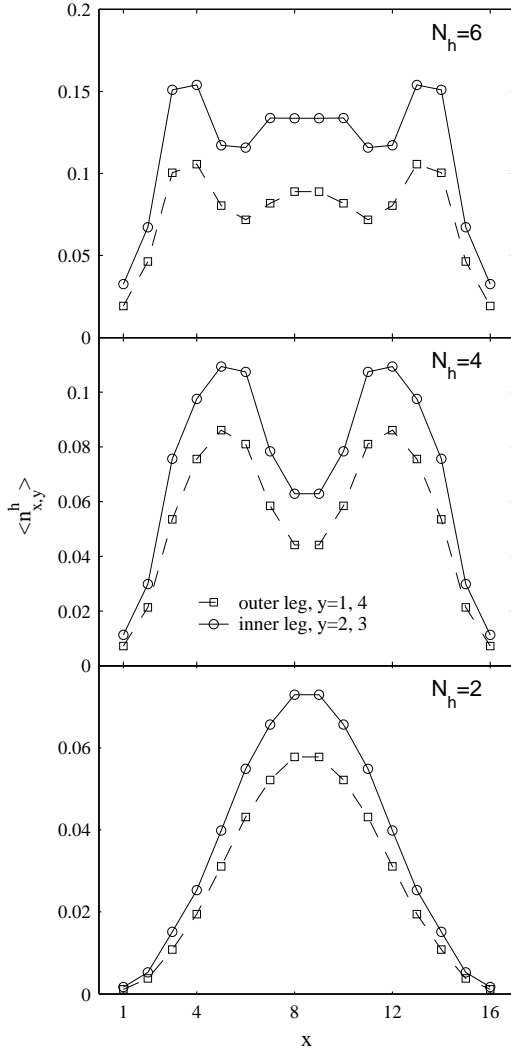
2

FIG. 3. Hole density profiles $\langle n_{x,y}^h \rangle$ on the inner and outer legs of a (16×4) t-J ladders with $J = 0.35\,t$ for $N_h = 2$, 4 and 6 holes doped into the ladder ($\delta < \frac{1}{8}$).
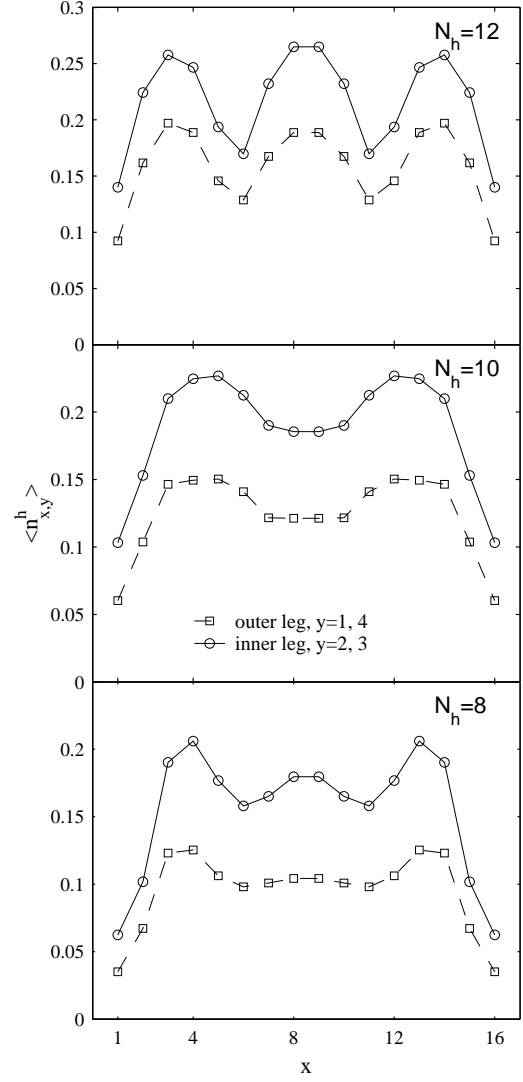
FIG. 4. Hole density profiles $\langle n_{x,y}^h \rangle$ on the inner and outer legs of a (16×4) t-J ladders with $J = 0.35\,t$ for $N_h = 8$, 10 and 12 holes doped into the ladder ($\delta \geq \frac{1}{8}$).
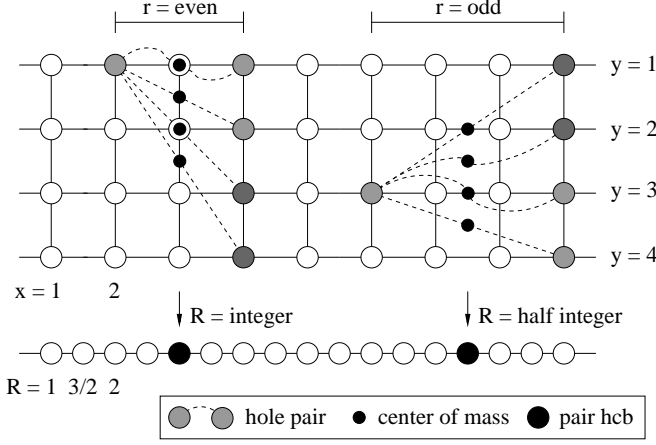
FIG. 5. Mapping of hole-pairs from a four-leg ladder to hard core bosons on a chain. The center of mass coordinate R of the hole-pair determines the hard core boson position.

III. LOW DENSITY OF HOLE-PAIRS

In this section we examine the t-J 4LL at low hole doping δ, i. e. $\delta < \delta_c$. In order to set up an effective bosonic model we first check the symmetry of the ground state at low hole dopings using a Lanczos method to get the lowest lying energy states with exact diagonalisation for a 6×4 t-J ladder with periodic boundary conditions along the legs. For 2 and 4 holes doped into the half filled ladder the ground state has even parity under reflection along and perpendicular to the legs.

Since the spin part of the ground state wavefunction is a singlet and thus antisymmetric and the spin excitations are gapped, [9] the charge degrees of freedom can be described by an even parity wavefunction where HP are considered as effective (hard core) bosons. At low hole dopings, $\delta < \delta_c$, only one HP is found on a rung. Hence, we can map HP in the $(L \times 4)$ t-J ladder with periodic boundary conditions in the long direction on HCB on a single closed chain as shown in Fig. 5. This effective model is completely analogous to the model for 2LL introduced in Ref. [12].

Since holes on a ladder can pair with more weight on adjacent rungs, our effective model incorporates the possibility that the "center of mass" of a HP can lie on a rung or between two rungs as shown in Fig. 5. Note that for even (odd) distance r along the legs between two holes, the center of mass lies on a rung (between two rungs). The HHC function $g(r)$ is connected to the probability of finding the center of mass of a pair on a rung, w_{int}, or between two rungs, w_{half}, by

$$w_{\text{int}} = \sum_{r_{\text{even}}} g(r) \tag{5}$$

$$w_{\text{half}} = \sum_{r_{\text{odd}}} g(r) \; .$$

The same occupation probabilities can be obtained with the one boson Hamiltonian

$$H_{\text{B}} = -t^* \sum_{R=\frac{1}{2}, 1, \ldots}^{L} (B_R^\dagger B_{R+\frac{1}{2}} + B_{R+\frac{1}{2}}^\dagger B_R) + \epsilon \sum_{R=\frac{1}{2}, \frac{3}{2}, \ldots}^{L} N_R \tag{6}$$

for a boson $B_R^\dagger$ which moves on a closed chain with length L, i. e. $2L$ sites, under the action of an alternating on-site potential which is 0 or ϵ on integer or half integer sites respectively. Here $N_R = B_R^\dagger B_R$ and $R = (1/2, 1, \ldots, L)$.

Figure 5 shows the mapping of HP from the ladder to effective bosons on a single chain. Note that the center of mass coordinate R of the pair determines the position of the effective boson. Here the ratio of the probabilities $w_{\text{half}}/w_{\text{int}}$ to find the boson on a site with half integer or integer R depends only on ϵ/t^* and can easily be obtained as

$$\frac{w_{\text{half}}}{w_{\text{int}}} = \frac{\epsilon^2 + (4t^*)^2 - \epsilon\sqrt{\epsilon^2 + (4t^*)^2}}{\epsilon^2 + (4t^*)^2 + \epsilon\sqrt{\epsilon^2 + (4t^*)^2}} \; . \tag{7}$$

From this equation and Eq. (5) we obtain for ϵ

$$\epsilon = 4\,t^* \sinh\left(\frac{1}{2}\,\ln\left|\frac{\sum_{r_{\text{even}}} g(r)}{\sum_{r_{\text{odd}}} g(r)}\right|\right) \; . \tag{8}$$

With $g(r) = g(r, R_0)$ obtained as explained in Sec. II for $R_0 \simeq L/2$ from a (32×4) t-J ladder we get $w_{\text{half}}/w_{\text{int}} = 1.18$ and $\epsilon = -0.33\,t^*$. This result shows that the HP is mainly centered between two rungs.

Once the boson density $\langle N_R \rangle$ for the model (6) has been computed, we obtain the hole rung density $\langle n_x^h \rangle = \sum_{y=1}^4 \langle n_{x,y}^h \rangle$ on rung x by the convolution

$$\langle n_x^h \rangle = \frac{1}{2} \frac{\sum_{r_{\text{even}}} g(r)(\langle N_{x-\frac{r}{2}} \rangle + \langle N_{x+\frac{r}{2}} \rangle)}{\sum_{r_{\text{even}}} g(r)}$$
$$+ \frac{1}{2} \frac{\sum_{r_{\text{odd}}} g(r)(\langle N_{x-\frac{r}{2}} \rangle + \langle N_{x+\frac{r}{2}} \rangle)}{\sum_{r_{\text{odd}}} g(r)} \; . \tag{9}$$

Next we generalize the one boson model to a finite density including the interactions between the HCB and also the effect of open boundary conditions and write the effective Hamiltonian for the HCB as

$$H_{\text{eff}} = H_{\text{B}} + V_{\text{int}} + V_{\text{b}} \tag{10}$$

The potential V_{int} gives the interaction between HCB, i. e. HP in the t-J model. Since the simulations are for finite systems, we have to take into account the interaction of the HP with the boundaries. The potential V_{b} has been introduced to describe this effect.

A. Computing V_{b} and V_{int}

Our procedure is to compute the HCB density $\langle N_R \rangle$, convolute it with $g(r)$ according to Eq. (9) and then to

4

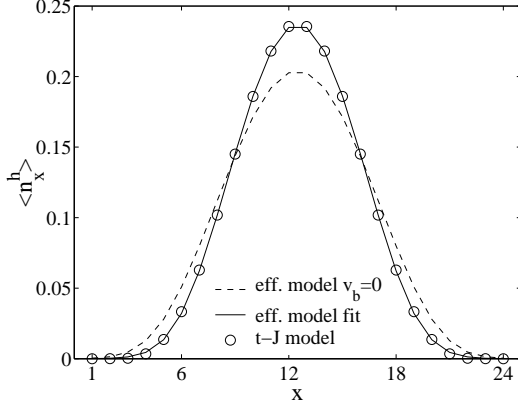FIG. 6. Hole rung density $\langle n_x^h \rangle$ for two holes on a (24×4) t-J ladder with $J = 0.35\,t$ computed directly and with the effective model using smooth boundary conditions. For the effective model the data for $v_b = 0$ and the best fit is shown.

compare it with the hole rung density $\langle n_x^h \rangle$ of the corresponding t-J system. In this way we obtain V_b and V_{int} by fitting the density profile of the effective model to that of the t-J model.

However there is a problem in the density profiles of the t-J ladders. The open boundary conditions induce density oscillations at the boundaries which cannot be neglected as in the case of the 2LL. [12] Due to the higher number of degrees of freedom the HP in the 4LL gets more distorted, when it approaches the open ends of the system. To circumvent this problem we use smooth bounday conditions (SBC) as proposed in Ref. [13] for both, the t-J and the effective model. The SBC introduce smoothly decreasing energy parameters into the Hamiltonian as the open ends of the ladder are approached. We use SBC only in the long direction which extend into the t-J ladder until the fifth rung from the open ends. We choose the same smoothing function as used in Ref. [14] for the Hubbard model. Details are explained in Appendix A.

We obtain V_b by considering one HP in the t-J model and choose an exponentially decreasing form for the potential term V_b

$$V_b = v_b \sum_R N_R \left(e^{-\frac{R-1}{\xi_b}} + e^{-\frac{L-R}{\xi_b}} \right) \tag{11}$$

with the two parameters v_b and ξ_b. Figure 7 shows the results of the fit and the optimal parameter values are displayed in Table I. Note that the rather large value of v_b is a consequence of the smoothing function, which also decreases the energy parameters of V_b, i.e. v_b, near the boundaries.

To obtain the interaction potential V_{int} we proceed in the same way as for V_b and choose a hard core form

$$V_{int} = \sum_R \sum_{R' > R} v_{int}(|R - R'|) N_R N_{R'} \tag{12}$$

TABLE I. Parameters for the boundary potential V_b given in Eq. (11) obtained from the density profile of a (24×4) t-J ladder for $J = 0.35\,t$.

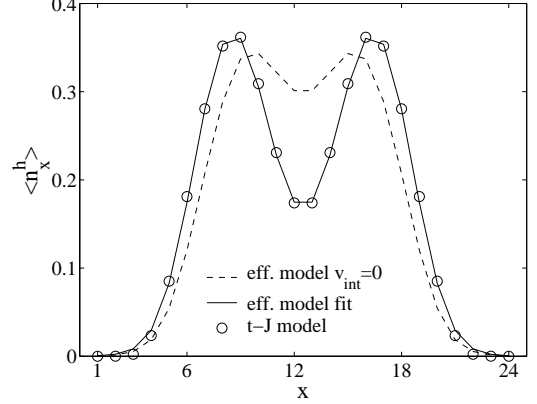| v_b/t^*	ξ_b
148×10^3	0.2980

FIG. 7. Hole rung density $\langle n_x^h \rangle$ for $J = 0.35\,t$ calculated for four holes on a (24×4) t-J ladder computed directly and with the effective model using smooth boundary conditions. For the effective model the data for $v_{int} = 0$ and the best fit is shown.

$$v_{int}(\Delta R) = \begin{cases} \infty & \Delta R < \Delta R_{min} \\ v_1 & \Delta R = \Delta R_{min} \\ v\, e^{-(R - R_{min} - \frac{1}{2})/\xi} & \Delta R > \Delta R_{min} \end{cases}.$$

We consider a (24×4) t-J ladder with four holes and the corresponding effective model with two HCB and use three fit parameters for the interaction potential and the additional parameter ΔR_{min}, which broadens the hard core of the bosons, to model the interaction between the pairs.

Using the fits to the density profiles as shown in Fig. 7 the parameter values quoted in Table II are obtained. Figure 9 shows the result together with that from Ref. [12] for the two leg ladder.

We have tested the results by comparing the density profiles for various numbers of HP and ladder lengths. We find good agreement between the density profiles obtained from the t-J model and the effective model for hole dopings $\delta \leq 0.08$, as can be seen from Fig. 8.

B. Luttinger liquid parameter K_ρ

Having determined the effective HCB model that describes the low energy properties of the HP in the t-J model, we can express the charge density and the super-
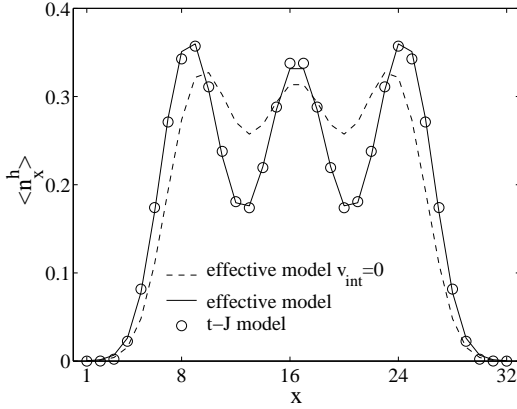
FIG. 8. Hole rung density $\langle n_x^h \rangle$ for $J = 0.35\,t$ for six holes on a (32×4) t-J ladder using smooth boundary conditions and computed with the interaction potential obtained from fits with two hole-pairs on 24×4 sites. The data for $V_{\text{int}} = 0$ for the effective model are also shown.

TABLE II. Parameters for the interaction potential V_{int} given in Eq. (12) obtained from the density profile of a (24×4) t-J ladder for $J = 0.35\,t$.

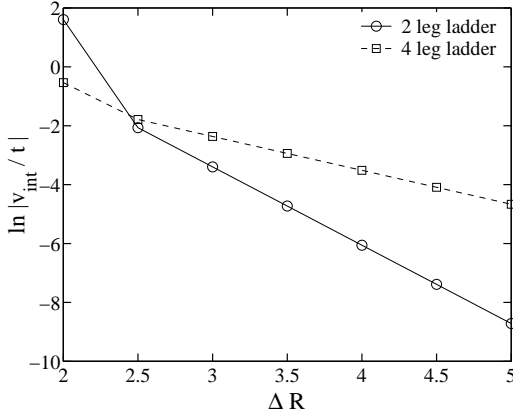| v_1/t^*	v/t^*	ξ	ΔR_{min}
0.5848	0.2978	0.8679	2

FIG. 9. Interaction parameter v_{int}/t from Eq. 12 obtained for the four-leg ladder in comparison with the result from the two-leg ladder from Ref. [12].
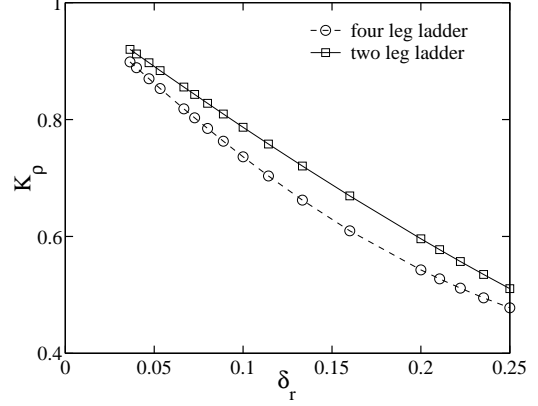

FIG. 10. Luttinger liquid parameter K_ρ as a function of hole doping for the four-leg t-J ladder in comparison with the results for the two-leg ladder from Ref. [12]. The hole doping is given in holes per rung, $\delta_r = N_l\,\delta$, with N_l as the number of legs.

conducting correlation functions in terms of Luttinger liquid parameter K_ρ as [15]

$$\langle N_R N_0 \rangle - \bar{N}^2 \sim \text{const} \times R^{-2} + \text{const} \times \cos(\pi(N_b/L)\,R)\,R^{-2K_\rho} \quad (13)$$
$$\langle B_R^\dagger B_0 \rangle \sim \text{const} \times R^{-1/2K_\rho} \quad , \quad (14)$$

with N_b as the number of HCB on the chain and $\bar{N} = N_b/2L$ the mean HCB density per site. These relations show that the superconducting correlations $\langle B_r^\dagger B_0 \rangle$ are dominant if $K_\rho > \frac{1}{2}$. For HCB in one dimension, K_ρ can be obtained from the relations [17]

$$K_\rho = \pi v_c N \left(\frac{\partial^2 E_0}{\partial N_b^2} \right)^{-1} \quad (15)$$
$$v_c K_\rho = \frac{\pi}{N} \left. \frac{\partial^2 E_0(\Phi)}{\partial \Phi^2} \right|_{\Phi=0} .$$

Here E_0 denotes the ground state energy for a closed ring of length L, i.e. $N = 2\,L$ sites, with N_b HCB and $E_0(\Phi)$ is the ground state energy of the system penetrated by a magnetic flux Φ which modifies the hopping by the usual Peierls phase factor, $t^* \mapsto t^* \exp(\pm i\Phi/N)$. From these two equations the charge velocity v_c can be eliminated. We used exact diagonalization for HCB chains with lengths between 32 and 220 and with $N_b = 2$.

The Luttinger liquid parameter K_ρ for the interaction potential given by the parameters in Table II approaches the universal value $K_\rho = 1$ at half filling. The results are shown in Fig. 10 where K_ρ is plotted as a function of the hole doping per rung in the corresponding t-J ladder, $\delta_r = 4\,\delta = 2\,N_b/N$. For $N_b/N \to 0$, corresponding to a very dilute HCB gas, we have $K_\rho = 1 + O(N_b/N)$ consistent with Ref. [18]. Up to $\delta \simeq 0.06$ ($\delta_r \simeq 0.23$) the superconducting correlations are dominant, since $K_\rho > \frac{1}{2}$.
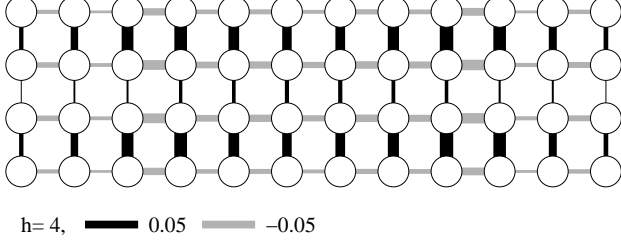
6

FIG. 11. Real space off diagonal singlet pairing expectation values $s^h_{\mathbf{i},\mathbf{j}}$ between nearest neighbor sites on a (12×4) t-J ladder for $h = 4$. The thickness of the lines gives the magnitude. Black and shaded lines denote positive and negative values respectively.

We have tested numerically the influence of the various parameters in Eq. 12 on K_ρ and v_c. A longer ranged interaction leads to a lower K_ρ and a larger v_c leaving the product $K_\rho v_c$ nearly unchanged. As Fig. 9 shows, the interaction between HP on 4LL is longer ranged than on 2LL. Accordingly, the Luttinger liquid parameter for the 4LL is lower in the investigated density range. As can be seen from Figure 10 the long range charge density wave correlations tend to overcome the superconducting correlations already at lower hole dopings with increasing dimensionality, i.e. when going from 2LL to 4LL.

IV. THE FORMATION OF FOUR HOLE CLUSTERS

In this section we examine the four-hole clusters (FHC) which form on a t-J 4LL at hole dopings higher than a critical doping $\delta_c \simeq \frac{1}{8}$.

First we clarify the question whether a change in the reflection symmetry occurs for the ground state wave function with increasing doping. We consider the real space off-diagonal singlet pairing expectation value (SPE) defined as

$$s^h_{\mathbf{i},\mathbf{j}} = \langle h - 2| c^\dagger_{\mathbf{i},\uparrow} c^\dagger_{\mathbf{j},\downarrow} - c^\dagger_{\mathbf{i},\downarrow} c^\dagger_{\mathbf{j},\uparrow} |h\rangle \qquad (16)$$

for nearest neighbor sites $\langle \mathbf{i},\mathbf{j}\rangle$. Here $|h\rangle$ denotes the ground state for h holes doped into the ladder. We have calculated the SPE on a 12×4 t-J ladder for h up to 12, i.e. a hole doping $\delta = \frac{1}{4}$. Figure 11 shows the results for $h = 4$. The SPE show a characteristic sign-pattern which would change with the reflection symmetry over the doping, i.e. when going from $h \to h + 2$. We observe no change as h is further increased and conclude that the ground state symmetry remains unchanged in the investigated density range. This result suggests that HP enter the same band at dopings below and above δ_c. Figure 11 reveals that at low hole doping HP enter in states where they reside predominantly on the outer 2LL since the magnitudes of the SPE between next neighbors
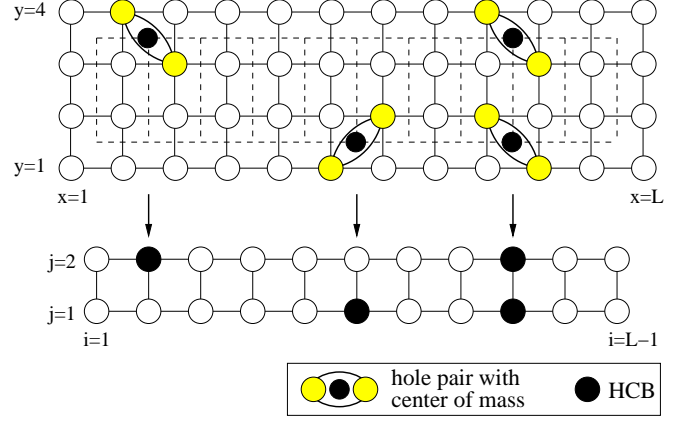

FIG. 12. Mapping of pairs of holes from a four-leg t−J ladder to hard core bosons on a two-leg ladder. In this representation a hole-pair is centered on a 2×2 plaquette on one of the two coupled two-leg ladders.

on these ladders are largest. But this does not imply that two holes sit on the same rung. Instead the HHC function $g_{y,y'}(x,x')$ shows that two holes can most probably be found in a diagonal configuration on a 2×2 plaquette on one of the two coupled 2LL.

To set up an effective model which can describe the formation of the FHC, we again model the charge degrees of freedom of HP by effective (hard core) bosons moving in a spin liquid but introduce additional transverse degrees of freedom by considering the t-J 4LL as two coupled 2LL. This allows us to map HP – represented by their center of mass – from the $(L \times 4)$ t-J ladder on HCB on a $((L - 1) \times 2)$ ladder as depicted in Fig. 12. In this representation a HP is centered on a 2×2 plaquette on one of the two coupled 2LL. The Hamiltonian is given by

$$H = -t_l \sum_{i=1}^{L-2} \sum_{j=1}^{2} (B^\dagger_{i,j} B_{i+1,j} + B^\dagger_{i+1,j} B_{i,j}) \qquad (17)$$

$$-t_r \sum_{i=1}^{L-1} (B^\dagger_{i,1} B_{i,2} + B^\dagger_{i,2} B_{i,1})$$

$$+\frac{1}{2} \sum_{i,j,i',j'} v(|i - i'|, |j - j'|) N_{i,j} N_{i',j'}$$

where $B^\dagger_{i,j}$ and $B_{i,j}$ create and destroy a HCB on site (i,j) respectively and $N_{i,j}$ is the corresponding density operator. The matrix elements t_l and t_r stand for nearest neighbor hopping along the legs and rungs of the 2LL. The last term describes the interaction between HP and is determined by the parameter $v(r_x, r_y)$ with r_x and r_y as the relative separation of two HCB along and perpendicular to the legs respectively.

As hopping matrix element along the legs, t_l, we use the value obtained in Ref. [12] for 2LL, $t_l = 0.303\,t$. The energy difference of the bonding and antibonding band is given by $2\,t_r$. We have computed this energy difference

TABLE III. Interaction parameter values $v(r_x, r_y)$ in units of the hopping matrix element t of the t-J Hamiltonian (1).

r_x	0	1	2	3	≥ 4
$v(r_x, 0)/t$	—	100	5	0.1	0
$v(r_x, 1)/t$	0	0.1	0.5	0.1	0

at wavevector $k_x = 0$ with exact diagonalisation for two holes on a 6×4 leg t-J ladder using periodic boundary conditions in the long direction and obtained $t_r = 0.092\,t$ so that $t_l/t_r \simeq 3$.

We are able to reproduce qualitatively the formation of FHC but the formation depends crucially on the form of the interaction between the HP. We know from Ref. [12] that on a 2LL HP repel each other and hence choose a repulsive interaction for $r_x > 0$ which tends to zero when r_x increases. Further we expect this repulsion to be less for hole pairs on different legs of the effective 2LL, i.e. $v(r_x, 1) < v(r_x, 0)$. At short distance we can expect a certain energy lowering due to a lower cost in magnetic energy in the configuration with four holes on neighboring sites. Thus we set the constraint that $v(r_x, 1)$ has a local minimum at $r_x = 0$.

The solution of the two particle problem for the effective HCB model with this type of interaction shows that in the ground state the two HCB are unbound. But there are also resonant cluster states which can be occupied at higher energies. Hence, it can be expected that with increasing HCB density beyond a certain value of the chemical potential a resonant state is occupied. This occurs when the expense in kinetic energy due to the loss of some degrees of freedom is compensated by a smaller interaction energy. Above the critical doping a HP can cluster with another on the same rung but then it tunnels from one suitable HP to another HP thereby gaining additional kinetic energy. A set of parameter values for $v(r_x, r_y)$ is given in Table III. With these we calculated the HCB density per rung, $\langle N_i \rangle = \sum_{j=1}^{2} \langle N_{i,j} \rangle$, for 3 up to 6 HCB on a 15×2 ladder shown in Fig. 13. These results correspond to the hole density profiles shown in Fig. 3 and Fig. 4 for the 16×4 t-J ladder for 3 up to 6 HP. As can be seen, the formation of FHC is reproduced qualitatively. The number of maxima in the density profiles does not change, if a fourth HCB (HP in the t-J model) is added and for 6 HCB (HP) we observe three well separated maxima, each containing two HCB (HP). The density profiles for 5 HCB and HP look a bit different. Here the two additional HP cluster with the others but, due to the repulsive interaction between them, they are pushed towards the open ends of the sample in x-direction. We observe the same effect in the effective model, where the two outer maxima have higher weights than the maxima in the center. We tested the effective model also for longer systems. Figure 14 shows the rung
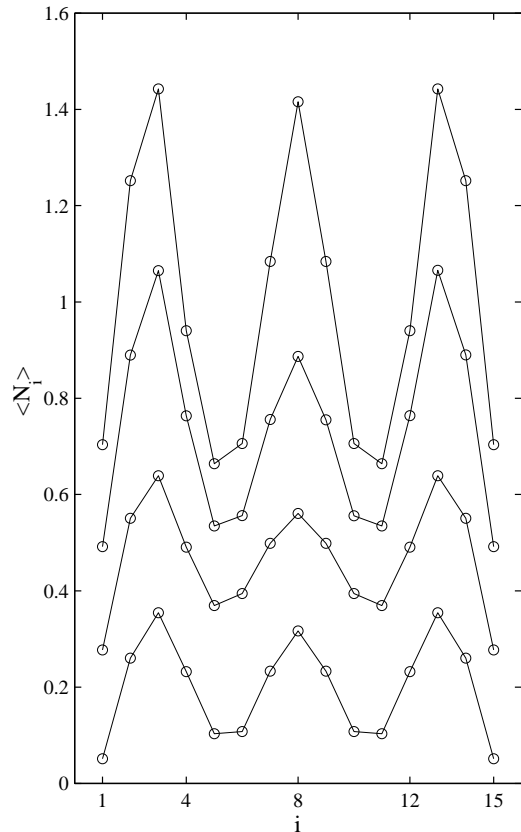

FIG. 13. Hard core boson (HCB) density per rung $\langle N_i \rangle$ obtained from the effective model (17) for a (15×2) ladder with 3 up to 6 HCB. From below: 3, 4, 5, and 6 HCB, respectively. The plots are shifted by 0.2 with respect to each other. The interaction parameter values from Table III have been used. The data reproduces qualitatively the hole cluster formation shown in Fig. 3 and Fig. 4.
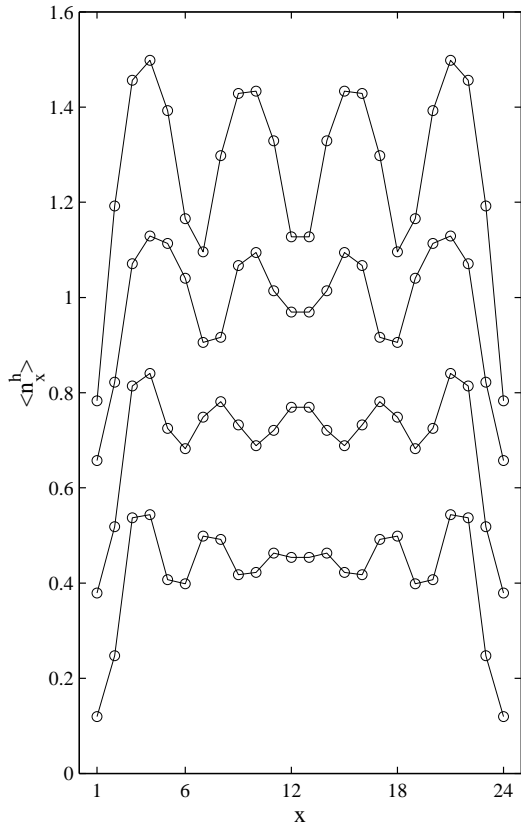
density profiles for 5 up to 8 HP on a (24×4) t-J ladder. The FHC start to form when going from 5 to 6 HP doped into the ladder, which corresponds again to a critical doping $\delta \simeq \frac{1}{8}$. By filling the ladder further with HP the number of maximum can also decrease. For 7 HP we observe only four maxima. The area attached to each maxima suggests that two FHC form near the open ends by occupying seven rungs each, whereas the remaining three HP share the inner ten rungs, where one pair is loosely bound with the other two. Finally, for 8 HP we observe 4 FHC which occupy 6 rungs each. Also this "contraction" of HP can be reproduced with the effective model using the interaction parameters from Table III. Figure 15 displays the corresponding rung density profiles for 5 up to 8 HCB on a 23×2 ladder. They show the same evolution with HCB number as the hole density profiles in Fig. 14 with HP number. We cannot expect the effective model to reproduce the behavior of the t-J model in all details, but in view of the simplicity of the model, the results are satisfactory. After scanning a wide parameter range for $v(r_x, r_y)$ we came to the conclusion that the formation of FHC can occur when the interaction leads to resonant states.

Since we observe a qualitative change in the density profiles, we have computed the chemical potential $\mu(h)$ of the HP as a function of hole doping

$$\mu(h) = E(h+1) - E(h-1) \qquad (18)$$

for both models in order to check whether it shows a singularity at the critical doping. Here, $E(h)$ denotes the ground state energy for a system with h holes or $h/2$ HCB in the t-J and effective model respectively. Figure 16 displays the chemical potential for HCB in the bosonic model for a 23×2 ladder as a function of the hole doping δ in the corresponding t-J model. The hole doping is related to the HCB number N_b by $\delta = N_b/2L$. The chemical potential shows a deviation from the quadratic form observed at low densities right at the position where the formation of the FHC sets in, i. e. when N_b is increased from 5 to 6. The exact position of this kink can be tuned by choosing appropriate interaction parameter values $v(r_x, r_y)$. The difference in the chemical potential between the critical and zero doping, $\Delta\mu \simeq 0.42\,t$, is to a good approximation given by the difference between the energies of the first resonant state and the ground state, $\Delta E = 0.43\,t$, obtained by solving the two particle problem. The critical doping can be shifted to lower values by making the interaction longer ranged. Figure 17 shows the chemical potential for hole pairs obtained from the corresponding 24×4 t-J ladder. The dashed dotted line shows a fit to a second order polynomial for $\delta < \delta_c$. As expected, the chemical potential $\mu(h)$ deviates from this polynomial for $\delta > \delta_c$.

Finally, we note that while the effective model reproduces the evolution of the system from HP to FHC nicely, it does not reproduce the density profiles quantitatively in the FHC density regime as can be seen, for example,
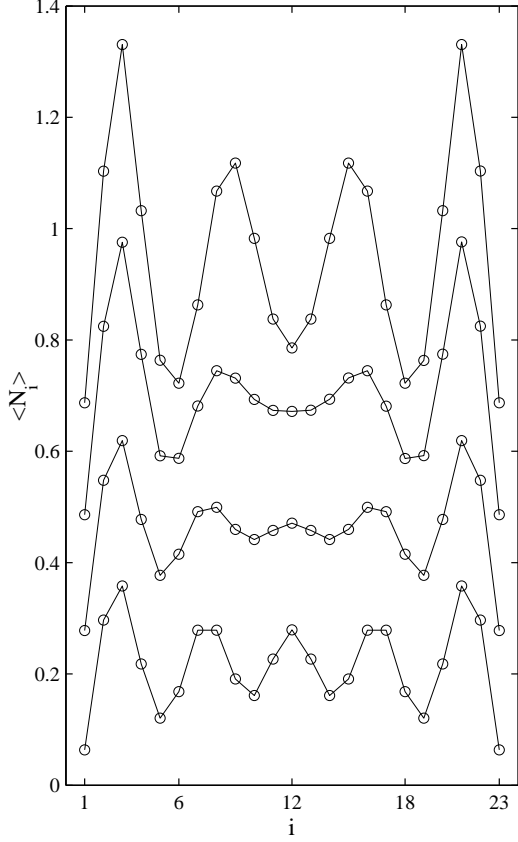

FIG. 14. Hole density per rung $\langle n_x^h \rangle$ on a (24×4) t-J ladder with $J = 0.35\,t$ for 5 up to 8 hole pairs doped into the ladder. From below: 5, 6, 7, and 8 hole pairs, respectively. The plots are shifted by 0.2 with respect to each other.

FIG. 15. Hard core boson (HCB) density per rung $\langle N_i \rangle$ obtained from the effective model (17) for a (23×2) ladder with 5 up to 8 HCB. From below: 5, 6, 7, and 8 HCB, respectively. The plots are shifted by 0.2 with respect to each other. The interaction parameter values from Table III have been used. The data reproduces qualitatively the hole cluster formation shown in Fig. 14.
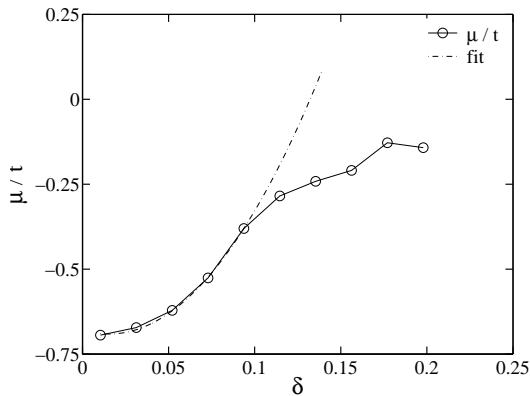

FIG. 16. Chemical potential μ/t for hard core bosons (hole-pairs) obtained from the bosonic model (17) for a (23×2) ladder using the interaction parameters from Table III as function of the hole doping δ in the corresponding t-J model. The dash-dotted line shows a fit to a second order polynomial in the region $\delta < \delta_c$.
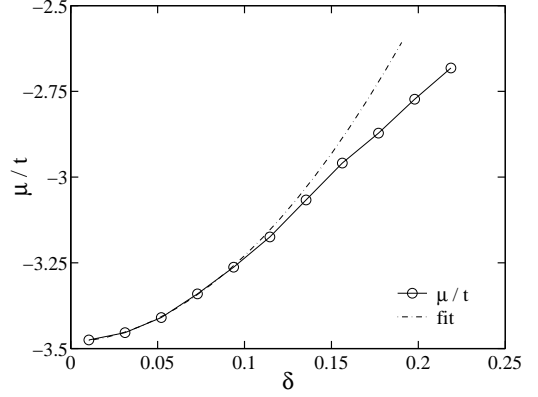

FIG. 17. Chemical potential μ/t for hole-pairs as a function of hole doping δ obtained for a (24×4) ladder with $J = 0.35\,t$. The dash-dotted line shows a fit to a second order polynomial in the region $\delta < \delta_c$.

by comparing the upper curves in Fig. 14 and 15. Therefore, further refinement of the effective model would be required to obtain the accuracy necessary to calculate parameters such as K_ρ from the effective model in this density regime.

V. CONCLUSIONS

In this work our previous study of the low energy properties of the hole doped t-J ladders with two legs is extended to the case of four legs. In both cases density matrix renormalization group (DMRG) results show that the holes bind in pairs at low densities and a finite spin gap is preserved. To analyze the DMRG results in more detail we introduce a hard core boson model on a single chain to describe the low energy degrees of freedom. The effective interactions between the hard core bosons which represent hole-pairs, are determined by fitting the density profiles to those obtained by DMRG methods for the t-J model. This effective repulsive interaction is longer ranged for the four-leg ladder and this in turn reduces the value of the Luttinger liquid parameter K_ρ. As a consequence the region of predominantly superconducting correlations is reduced in the wider ladder. Whereas the hole-pairs in the two-leg ladder simply repel each other, in the wider four-leg ladder a modification of the hole density profiles appears beyond a critical hole doping which can be simply interpreted as the formation of four hole clusters. To reproduce this behavior in the hard core boson model, it is necessary to introduce an extra transverse degree of freedom by replacing the single chain with a two-leg ladder. It is also necessary to modify the interaction potential to incorporate a four hole cluster as a finite energy resonance. This is achieved by replacing the monotonically decreasing repulsive interaction on the single chain by one with a potential minimum at short
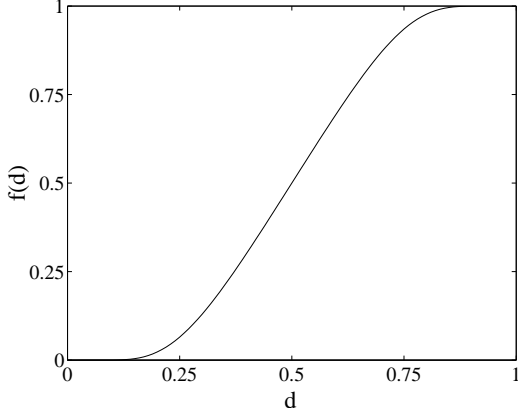
FIG. 18. Smoothing function $f(d)$. The parameter d gives the distance to the nearest outermost rung of the system in units of the width m of the boundary.

range. The longer range repulsive tail of the interaction potential causes the chemical potential to add a hole-pair to rise as the density is increased. When the chemical potential exceeds a critical value approximately equal to the resonance energy, the four hole clusters are formed leading to a kink in the chemical potential as a function of hole density.

VI. ACKNOWLEDGEMENTS

APPENDIX A: SMOOTH BOUNDARY CONDITIONS

The SBC introduce smoothly decreasing energy parameters into the Hamiltonian as the edges of the lattice are approached. [13,14] The result of this operation is that, instead of having a sharp and rigid boundary, the boundary extends itself into the system and its exact size is not fully determinable. In this way we talk of the bulk of the system as the region where the energy parameters are constant, and of the boundary as the region over which the parameters are smoothly turned off.

For the t-J ladders we use SBC only in the long direction and denote the width of the boundary with m. By applying SBC to the Hamiltonians (1) and (6) we replace the energy parameters t, J, t^*, ϵ, $v_{\rm b}$, and $v_{\rm int}$ by the site dependent parameters $t_{\bf i,j}$, $J_{\bf i,j}$, t_R^*, ϵ_R, $v_{{\rm b},R}$, and $v_{{\rm int},R,R'}$ respectively. All these parameters are scaled according to the smoothing function f defined as

$$f(d) = \begin{cases} 0 & d = 0 \\ \frac{1}{2}\left[1 + \tanh\frac{d-\frac{1}{2}}{d(1-d)}\right] & 0 < d < 1 \\ 1 & d >= 1 \end{cases} \quad \text{(A1)}$$

and plotted in Fig.18. Here d denotes the distance to the nearest outermost rung of the system in units of m. For the t-J model we use

$$d_{\bf i,i'} = d_{x,y,x',y'} = \min(\frac{x + x'}{2} - 1, L - \frac{x + x'}{2})/m \quad \text{(A2)}$$

with L as the number of sites in the long direction of the t-J ladder and scale the energy parameters in such a way that $t_{\bf i,j}/t = f(d_{\bf i,j})$ and $J_{\bf i,j}/J = f(d_{\bf i,j})$, where t and J are the bulk values.

For the one dimensional chain with length N of the effective model we define

$$d_{R,R'} = \min(\frac{R + R'}{2} - 1, N - \frac{R + R'}{2})/m \quad \text{(A3)}$$
$$d_R = \min(R - 1, N - R)/m$$

and scale the energy parameters in the way that $t_R^*/t^* = f(d_{R+\frac{1}{4}})$, $\epsilon_R/\epsilon = f(d_R)$, $v_{{\rm b},R}/v_{\rm b} = f(d_R)$, and $v_{{\rm int},R,R'}/v_{\rm int} = f(d_{R,R'})$. Here again, t^*, ϵ, $v_{\rm b}$, and $v_{\rm int}$ are the bulk values.

To determine an appropriate value for the width m of the boundaries we have considered the curvature of the rung hole density profile of a (24×4) t-J ladder. For $m < 4$ the curvature is far from being a smooth function of the rung coordinate but for $m = 4$ it is. So we have used $m = 4$ for the computations with SBC.

[1] S. R. White, Phys. Rev. Lett. **69**, 2863 (1992).
[2] S. R. White, Phys. Rev. B **48**, 10345 (1993).
[3] E. Dagotto, J. Riera, and D. Scalapino, Phys. Rev. B **45**, 5744 (1992).
[4] T. Barnes, E. Dagotto, J. Riera, and E. S. Swanson, Phys. Rev. B **47**, 3196 (1993).
[5] R. M. Noack, S. R. White, and D. J. Scalapino, Phys. Rev. Lett. **73**, 882 (1994).
[6] S. R. White, R. M. Noack, and D. J. Scalapino, Phys. Rev. Lett. **73**, 886 (1994).
[7] S. Gopalan, T M. Rice, and M. Sigrist, Europhys. Lett. **23**, 445 (1993).
[8] H. Tsunetsugu, M. Troyer, T. M. Rice, Phys. Rev. B **49**, 16078 (1994).
[9] M. Troyer, H. Tsunetsugu, T. M. Rice, Phys. Rev. B **53**, 251 (1996)
[10] E. Dagotto and T. M. Rice, Science **271**, 618 (1996).
[11] F. C. Zhang, T. M. Rice, Phys. Rev. B **37**, 3759 (1988).
[12] Thomas Siller, Matthias Troyer, T. M. Rice, S. R. White, Phys. Rev. B **63**, 195106 (2001)
[13] M. Vekić, S. R. White, Phys. Rev. Lett. **71**, 4283 (1993)
[14] M. Vekić, S. R. White, Phys. Rev. B **53**, 14552 (1996)

[15] A. Luther and I. Peschel, Phys. Rev. B **12**, 3908 (1975)

[16] F. D. M. Haldane, Phys. Rev. Lett. **45**, 1358 (1980)

[17] H. J. Schulz, Phys. Rev. Lett. **64**, 2831 (1990)

[18] H. J. Schulz, Phys. Rev. B. **59**, R2471 (1999)